Efficient Second Harmonic Generation of a Diode-Laser-Pumped CW Nd:YAG Laser Using Monolithic $MgO:LiNbO_3$ External Resonant Cavities

WILLIAM J. KOZLOVSKY, C. D. NABORS, AND ROBERT L. BYER, FELLOW, IEEE

Abstract—**We report 56% efficient external cavity resonant second harmonic generation of a diode-laser pumped, CW single-axial-mode Nd:YAG laser. A theory of external doubling with a resonant fundamental is presented and compared to experimental results for three monolithic cavities of nonlinear $MgO:LiNbO_3$. The best conversion efficiency was obtained with a 12.5 mm long monolithic ring cavity doubler, which produced 29.7 mW of CW, single axial mode 532 nm radiation from an input of 52.6 mW.**

I. Introduction

THERE has been increasing interest in the development and applications of diode-laser-pumped solid-state lasers. Diode-laser-pumped lasers offer improved reliability, efficiency, and frequency stability [1] compared to lamp-pumped lasers. An important application of diode-laser-pumped solid-state lasers is in the generation of visible radiation by frequency doubling [2]. Since the diode-pumped CW laser power levels are relatively low, efficient second harmonic generation (SHG) requires some method of increasing the intensities in the doubling crystal. Approaches to CW nonlinear conversion have concentrated on intracavity frequency doubling [3], intracavity sum generation [4], and self-frequency doubling [5] where advantage is taken of the high circulating intensity present inside the laser resonator. Although these internal SHG lasers yield good conversion efficiencies, they usually oscillate in several axial modes, resulting in large amplitude fluctuations at the second harmonic [6].

An approach that circumvents this problem, the use of an external resonance cavity to enhance the fields present in the doubling crystal, was first demonstrated by Ashkin *et al.* in 1966 [7]. This approach allows the laser cavity and the external resonance cavity to be independently optimized, which is especially important in low gain or quasi-three-level laser systems [8], [9]. Independent optimization also allows the design of a single axial mode laser source [10], thus ensuring that the output of the external doubler is also in single frequency.

External cavity resonant SHG experiments have been reported by a number of investigators. Ashkin *et al.* reported an enhancement of 2–3 of the fundamental in the doubling crystal over the case where no resonator was used, and concluded that their lossy (4 percent single-pass) KDP crystal and the noise in their laser prevented them from achieving better results. Further efforts in external cavity resonant doubling have been carried out using frequency-stable dye and argon ion lasers. Brieger *et al.* reported a fundamental enhancement of 15 in an external ring cavity containing an ADA crystal and having 6.6 percent roundtrip losses [11]. Continuous wave, ring cavity resonant doubling using ADP has been reported on by Bergquist *et al.* to generate high-power UV output [12]. When the ADP crystal was placed in a cavity of 3 percent roundtrip loss, enhancements of approximately 20 of the fundamental power resulted. Baumert *et al.* reported using $KNbO_3$ in an external cavity to frequency double the output of a low-power (55 mW) dye laser [13]. The fundamental enhancement of 6 resulted in a 1.5 percent conversion efficiency and was also limited by cavity losses.

The results of earlier investigators have indicated the importance of both frequency stable lasers for maintaining the resonance condition, and the use of very low-loss external cavities and doubling crystals for large fundamental enhancements. An important advance in making resonant SHG possible for diode-laser-pumped solid-state lasers has been the recent development of monolithic nonplanar ring geometries in Nd:YAG that produce frequency-stable single-mode outputs [10], [14]. The other important advance used for these experiments was the development of high-quality $MgO:LiNbO_3$ as a nonlinear material, which has a loss of 1064 nm of less than 0.003 cm^{-1} [15]. In addition, the material does not suffer from photorefractive effects when frequency doubling 1064 nm light at the 107°C phase-matching temperature.

Manuscript received December 8, 1987. This work was supported by the U.S. Army Research Office under Grant DAAG 29-84-K-0071 and by NASA under Grant NAG-1-182. The work of W. J. Kozlovsky and C. D. Nabors was supported by the Fannie and John Hertz Foundation.

The authors are with the Edward L. Ginzton Laboratory, Stanford University, Stanford, CA 94305.

IEEE Log Number 8820463.

0018-9197/88/0600-0913$01.00 © 1988 IEEE

II. Theory

The SHG conversion efficiency of an external cavity doubler may be determined from the theory of Ashkin, Boyd, and Dziedzic (ABD) [7]. Fig. 1(a) and (b) show the two monolithic doubling cavity geometries used for our experiments: (a) the standing wave, and (b) the ring configuration. Note that the standing wave cavity is phase matched for both the forward and backward propagating intracavity beams, resulting in two second harmonic outputs. The ring geometry is phase matched only for the forward beam, and therefore generates second harmonic in a single direction. Following the notation of ABD, let r_1 and r_2 be the power reflection coefficients of the cavity mirrors M_1 and M_2, and let t_1 and t_2 be their power transmission coefficients. The mirrors are assumed to be lossless, so that $r_1 + t_1 = r_2 + t_2 = 1$. Any real scatter losses in the mirrors can be included in t, the single-pass power transmission coefficient of the material in the resonator. P_1 is the fundamental power incident on the cavity and P_r is the fundamental power reflected from the cavity. P_c is the circulating fundamental power just inside the first mirror M_1 of the external resonator. The crystal transmission and the mirror reflectivities are assumed to be nearly unity, so that the circulating power may be approximated as being constant throughout the crystal.

For very low-loss resonators and crystals, it is useful to extend the theory of ABD to take into account depletion of the resonated fundamental due to the doubling process. As long as this "loss" of the circulating power to the second harmonic remains small, it can be described by an additional crystal transmission term t_{SH}. Let

$$t_{SH} = (1 - \gamma_{SH} P_c) \tag{1}$$

be the fraction of resonated fundamental not frequency doubled in a single pass through the crystal where

$$\gamma_{SH} P_c = \eta_{SH} \tag{2}$$

is the conversion efficiency of the resonated fundamental to the second harmonic.

The nonlinear conversion factor γ_{SH} can be derived using the formalism of Boyd and Kleinman for a focused Gaussian beam [16]. For an interaction length L in a crystal of index n with an effective nonlinear coefficient d_{eff} [17],

$$\gamma_{SH} = \left(\frac{2\omega^2 d_{\text{eff}}^2 k_\omega}{\pi n^3 \epsilon_0 c^3} \right) Lh(B, \xi) \tag{3}$$

where ω is the laser fundamental frequency, k_ω is the fundamental wavenumber n is the index of refraction of the crystal, c is the speed of light, and ϵ_0 is the permittivity of free space. $h(B, \xi)$ is the Boyd and Kleinman focusing factor, with the double refraction parameter B and focusing parameter ξ. For noncritical (90°) phase matching, there is no walkoff and $B = 0$. The focusing parameter for a spot size of w_0 is $\xi = L/w_0^2 k_\omega = L/b$ for confocal parameter b. The nonlinear conversion factor for $MgO:LiNbO_3$, with a $d_{\text{eff}} = 5.95 \times 10^{-12}$ m/V and an $n = 2.23$ for doubling 1064 nm radiation [18], is $\gamma_{SHG} = 0.35Lh(0, \xi)$ for L expressed in meters.

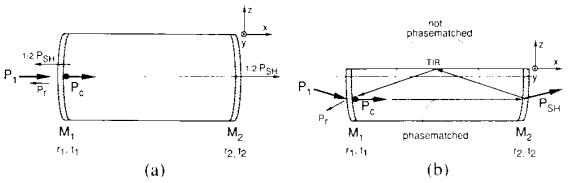

Fig. 1. Monolithic resonators: (a) standing wave geometry, (b) ring geometry. The mirrors, reflecting at the fundamental and transmitting at the second harmonic, are applied directly to the polished crystal ends.

As in ADB, the resonated fundamental and therefore second harmonic output can be solved for in terms of the crystal transmission and cavity mirror characteristics. It is useful to define a term r_m, the cavity reflectance parameter, which represents the fraction of resonated fundamental left after one roundtrip inside the cavity. For the ring cavity, which generates green in only one direction, the cavity reflectance parameter becomes

$$r_m = t^2 t_{SH} r_2. \tag{4a}$$

For the standing wave geometry, which generates green in both directions,

$$r_m = t^2 t_{SH}^2 r_2. \tag{4b}$$

The significance of the cavity reflectance parameter can be seen in the expression for the reflected fundamental power. On resonance,

$$\frac{P_r}{P_1} = \frac{\left(\sqrt{r_1} - \sqrt{r_m}\right)^2}{\left(1 - \sqrt{r_1 r_m}\right)^2}. \tag{5}$$

If $r_1 = r_m$, then $P_r = 0$ and all of the incident power is coupled into the external cavity. Choosing this mirror reflectivity "impedance matches" the resonator. Since r_m depends on P_c through t_{SH}, this impedance matching condition is dependent on the incident power level and on the doubling efficiency.

The enhancement of the fundamental power on resonance is given by

$$\frac{P_c}{P_1} = \frac{t_1}{\left(1 - \sqrt{r_1 r_m}\right)^2}, \tag{6}$$

which also determines the circulating power. Due to the dependence of r_m on the circulating power, (6) is a cubic equation in P_c. This is easiest to solve numerically for the specific system and power level of interest. The expected second harmonic output is determined by P_c. For the ring geometry,

$$P_{SH} = \gamma_{SH} P_c^2. \tag{7a}$$

For the standing wave geometry,

$$P_{SH} = 2\gamma_{SH} P_c^2, \tag{7b}$$

which represents the sum of the forward and backward propagating second harmonic outputs. The overall conversion efficiency is given by P_{SH}/P_1.

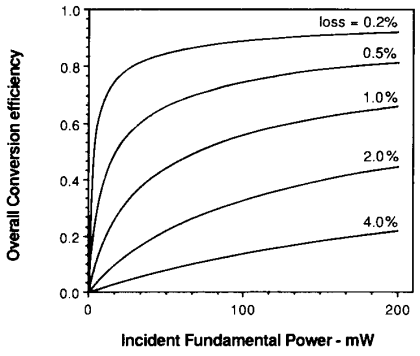

Fig. 2. Dependence of conversion efficiency on roundtrip cavity losses ($1 - t^2$). Perfect impedance matching is assumed at each incident power level with an $r_2 = 1$. A 1 cm $LiNbO_3$, confocally focused ($\xi = 1$) ring geometry is assumed, yielding $\gamma_{SHG} = 0.0028/W$.

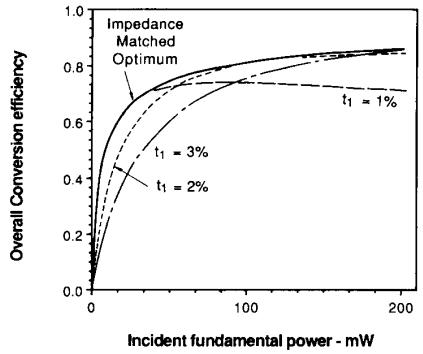

Fig. 3. Effect of increasing conversion on the impedance matching condition. The output of a 1 cm $LiNbO_3$, confocally focused ($\xi = 1$) ring geometry of $t = 0.997$ is plotted for various fixed incoupler t_1 values and compared to the impedance matched optimum.

The importance of using low-loss crystals with properly impedance matched resonators is seen by using the above equations in a numerical example. Fig. 2 shows the maximum conversion efficiency expected for a monolithic ring external doubler for various levels of roundtrip loss (defined as $1 - t^2$) as a function of input power where perfect impedance matching is assumed at all input powers. Since operation at a specific r_1 is necessary for monolithic devices, perfect impedance matching is only possible at a particular power level. Fig. 3 shows the output powers expected for particular input mirror reflectivities as a function of input power as compared to the impedance-matched optimum. It should be noted that although the conversion efficiency peaks for each specific r_1, the second harmonic power still increases monotonically as a function of input power.

III. Experiments

The Nd:YAG nonplanar ring oscillator used in these experiments has been described elsewhere by Kane *et al.* [19]. The laser operated TEM_{00} and in a single axial mode with a linewidth of less than 10 kHz and a drift of less than 1 MHz/min. This frequency stability is well within the linewidth of the doubling cavities considered here (6–18 MHz), and so laser linewidth effects can be safely ignored. The laser produced 15 mW of CW output power when pumped by a 120 mW diode laser. This laser was used for the standing wave external resonator experiment. The same laser geometry with a greater outcoupling produced 53 mW of single axial mode output when pumped with a 500 mW diode laser. This higher power laser was used for the ring cavity doubler experiments.

$MgO:LiNbO_3$ was selected as the nonlinear material for these experiments because of its low loss and large nonlinear coefficient for noncritical phase-matched doubling of 1064 nm radiation. The one uncertain parameter for the material was the maximum length of crystal that could be phase matched. Previous work has shown that the phase-matching length is limited to approximately 12 mm due to the MgO concentration gradient down the length of the boule [15]. Choosing both the crystal growth direction and the propagation direction along the x axis was necessary to avoid scattering from striae that arise during growth from the noncongruent melt.

A monolithic cavity was desired for these experiments to ensure the lowest possible cavity losses and good frequency stability. The resonators were formed by polishing curved ends on the $MgO:LiNbO_3$ crystal and then depositing thin film coatings directly on these curved surfaces. To fabricate a ring cavity, the z face of the crystal was polished parallel to the mirror axes, resulting in an off-axis ring such as shown in Fig. 1(b). Using $MgO:LiNbO_3$ allowed the resonator's optical length to be controlled electrooptically with the r_{22} coefficient by applying a voltage across the y axis of the crystal. By applying a linear ramp voltage and detecting the transmitted fundamental power when the crystal was not at the phase-matching temperature, we measured the finesse of the external resonator. Knowledge of the finesse enabled the cavity losses to be determined, which are important for fitting the experimental results to the theory.

The experiments were performed on three separate monolithic resonators. The characteristics of these resonators are given in Table I. The results of the first crystal resonator, a standing wave geometry doubler, have been previously published [20] and are summarized here. Fig. 4 shows the experimental setup used for the standing wave doubler experiment. The laser output was collimated with a lens of focal length 60 mm and then carefully spatially mode matched into the external cavity as discussed by Kogelnik and Li [21] with a lens of focal length of 100 mm. When the monolithic standing wave resonator was placed in an oven and heated to the phase-matching temperature of 107°C, second harmonic was generated in both directions. Dichroic beam splitters allowed both outputs to be measured. A Faraday isolator was used to collect the light reflected from the crystal cavity. This reflected light was minimized on resonance, and so was used as a feedback signal to lock the external cavity to the laser frequency. To accomplish this locking, the crystal voltage

TABLE I
PARAMETERS OF MONOLITHIC EXTERNAL CAVITY FREQUENCY DOUBLING CRYSTALS

	FSR Scanning Voltage (Volts)	Finesse	r_1	r_2	t^2 (roundtrip transmission)	w_0 (spot size) (μm)	γ_{SH} (W^{-1})
Standing wave doubler x-axis length = 25 mm y-axis width = 4 mm FSR = 2.7 GHz mirror radii = 20 mm	1040	450	0.997	0.997	0.992	38	0.0025
Ring doubler x-axis length = 25 mm y-axis width = 2.5 mm FSR = 2.7 GHz mirror radii = 20 mm	650		0.983	0.9996	0.992	38	0.0025
Ring doubler x-axis length = 12.5 mm y-axis width = 2.2 mm FSR = 5.4 GHz mirror radii = 10 mm	1150	292	0.983	0.9996	0.9958	27	0.0039

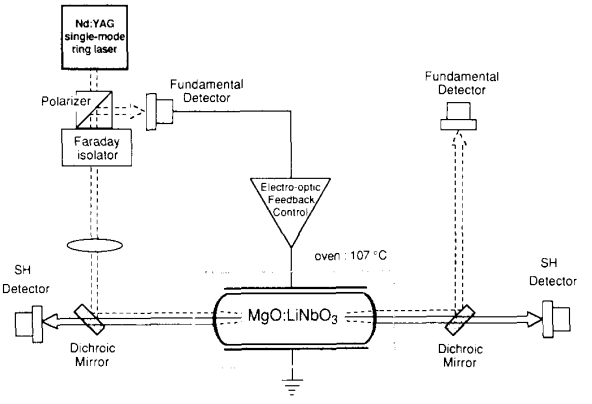

Fig. 4. Experimental setup for the standing wave geometry doubler. The dichroic mirrors allow measurement of both second harmonic outputs. The Faraday isolator allows detection of the fundamental power back-reflected from the doubling cavity for locking on resonance.

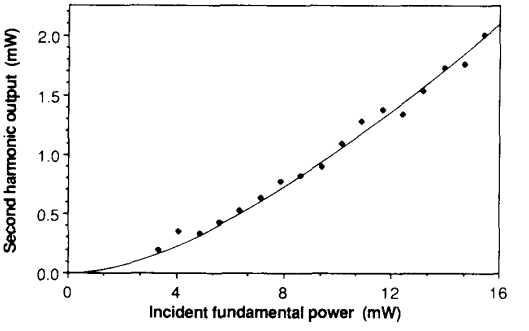

Fig. 5. Standing wave resonant doubler results. The output plotted is the total power (the sum of the two outputs). The dots are experimental points; the line is the theory.

had a small dither (at 7.2 kHz) applied to it. A lock-in amplifier with 3 Hz filter bandwidth was used to detect this component on the reflected light, and the resulting dispersive-shaped signal was fed through a PI servo amplifier and then to the high-voltage amplifier.

Fig. 5 shows the output of this standing wave external resonant SHG device. The maximum fundamental power available for this experiment was 15 mW due to diode pump limitations. At this level of input, a total of 2 mW of second harmonic was generated for a total conversion efficiency of 13 percent. The data compare well to the theory when the phase-matchable length L was adjusted to $L = 13$ mm. This length gives an $Lh(0, \xi) = 7 \times 10^{-3}$ so that $\gamma_{SHG} = 0.0025/W$. Measuring the transmitted fundamental power allowed determination of the resonator's circulating power. At an incident power of 15 mW, the circulating power was 600 mW, representing an enhancement of 40 in the fundamental. At this power level, though, 2 mW was transmitted through the resonator and 6 mW was back reflected. This was due to the 99.7 percent mirror reflectivities, which leaked circulating power through mirror M_2 and did not provide proper impedance matching at mirror M_1.

The second external SHG crystal resonator was fabricated with the same length and mirror curvatures as the standing wave doubler. To fabricate a ring resonator, such as shown in Fig. 1(b), the z face of the crystal was polished down to 0.25 mm from the axis of the mirrors. The thickness of the crystal across the y axis was reduced to lower the interferometer FSR scanning voltage. A 98.3 percent reflector at 1.06 μm was deposited as mirror M_1 to better couple the fundamental into the cavity. A high reflector (at 1064 nm) was deposited as M_2, which measured 0.04 percent transmitting at the fundamental and 85 percent transmitting at the second harmonic.

Since the $MgO:LiNbO_3$ crystal was determined to be phase matching over an effective length of only 13 mm, the third crystal was fabricated 12.5 mm in length. The z face was polished to 0.18 mm from the axis of the mirrors to complete the ring. The output high reflector and the input 98.3 percent reflector coatings were identical to those on the previous crystal. The measured finesse of 292 for this crystal indicated that the total scatter and absorption losses were 0.42 percent at the fundamental.

Fig. 6 shows the experimental setup for the external ring resonant doubler experiments. The ring geometry eliminates the need for a Faraday isolator since the incident fundamental is not retroreflected from the external cavity. This reflected power is detected and used for locking on resonance. The dither and lock-in detection technique discussed above was used for all the data presented here, but locking of the external crystal cavity was also demonstrated using both the Hänsch–Couillaud polarization spectroscopy technique [22] and Pound–Drever FM spectroscopy technique [23]. For the Hänsch–Couillaud technique, the polarization anisotropy of the crystal itself was used as an intracavity polarizing element. The Pound–Drever technique used FM sidebands generated inside the electrooptic crystal resonator by applying RF power through a bias tee, rather than using an external phase modulator.

The amplitude noise spectrum of the fundamental and the second harmonic were measured for the 12.5 mm ring doubler. The 8 percent (peak-to-peak) noise in the doubler output at full power was principally due to 3 percent noise in the laser output with additional noise from the servoloop. Spectrum analyzer traces of both the laser and doubler output showed sharp noise peaks at the 320 kHz relaxation oscillation frequency of the laser, with the doubler noise about 5 dB greater (3 dB is expected from theory). The laser noise, dominated by relaxation oscillations in the Nd:YAG nonplanar ring oscillator, was attributed to the diode laser pump power fluctuations. The long-term frequency stability of the doubler output is determined by the laser stability since the doubler cavity is servoed to the laser output. The laser frequency was controlled by temperature tuning the laser crystal, with a tuning coefficient for the monolithic Nd:YAG laser of -3.1 GHz/°C.

We measured the temperature tuning coefficient for monolithic $MgO:LiNbO_3$ resonators to be -4.4 GHz/°C. The large fundamental field buildup in the external cavity caused heating due to absorption, pushing the resonance approximately 1/3 of a FSR. The dither/lock-in detection servo proved to be very robust, tracking this effect, and the system maintained lock and good second harmonic power stability for arbitrarily long periods. The effect of space-charge screening of the applied field by photoconductive electrons [24] seemed negligible.

Fig. 7 shows the output of the 25 mm crystal ring cavity as a function of incident power. The crystal generated 18 mW of second harmonic at an incident power of 45 mW for a conversion efficiency of 40 percent. At this power level, the cavity reflected only 5 percent of the incident power and transmitted 2 percent. Since the incoupler was chosen to impedance match at this power level, the residual 5 percent reflection was attributed to imperfect spatial mode matching caused the slight astigmatism of both the laser and doubler cavity designs. The theoretical curve was generated using the same 0.8 percent roundtrip cavity loss and effective length of $L = 13$ mm that was used in the first crystal, and taking into account the imperfect

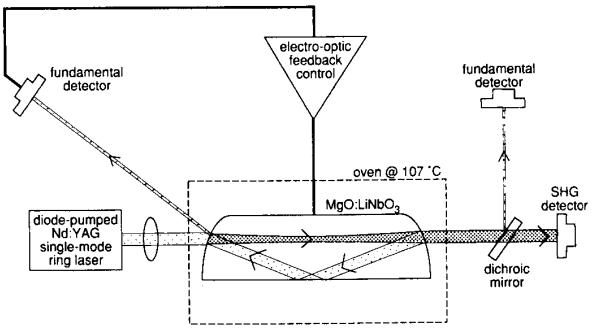

Fig. 6. Experimental setup for the ring geometry doubler. The single-ended output is detected through the dichroic mirror. The reflected fundamental used for locking is measured directly, eliminating the need for a Faraday isolator.

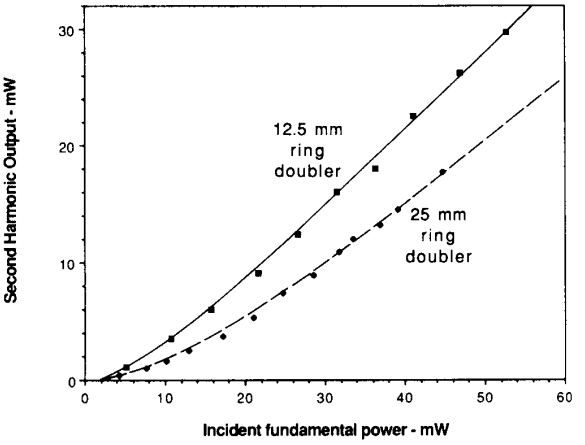

Fig. 7. Ring resonant doubler output. The dots are experimental points; the line is the theory. The 25 mm long ring cavity has 20 mm radii of curvature mirrors, and a 13 mm phase-matchable length. The 12.5 mm long ring cavity has 10 mm radii of curvature mirrors.

coupling and the 15 percent loss of the second harmonic at mirror M_2 (bireflection prevents the reflected green light from being reentrant). The second harmonic generated represented a loss of the circulating power of only 0.7 percent, on the same order as the scatter and absorption losses, and that the enhancement of the incident fundamental power was 53.

Fig. 7 also shows the output of 12.5 mm ring doubler. The crystal generated 29.7 mW of 532 nm power from an incident fundamental power of 52.7 mW for a 56 percent conversion efficiency. At this level of incident power, the crystal transmitted 2 percent and reflected 7.5 percent of the incident light. This larger level of reflected light as compared to the 25 mm cavity is probably due to the larger astigmatism and smaller spot size for this cavity. The theoretical output of the doubler is also plotted in Fig. 7, using the measured losses and a phase-matching length of 12.5 mm. The imperfect coupling and the 15 percent loss of the second harmonic at the exit face of the crystal is again accounted for in the theoretical calculation. The cavity parameters give an $Lh(0, \xi) = 1.13 \times 10^{-2}$.

Therefore, this shorter crystal, with its smaller waist and full phase-matched length, has a $\gamma_{SH} = 0.0039/\mathrm{W}$. At the 52 mW incident power, the circulating fundamental power was 3000 mW, which represents an enhancement of 60 for the fundamental. The loss of the circulating power to the second harmonic was 1 percent, much more than the 0.42 percent scatter and absorption losses.

It should be noted that the 56 percent conversion efficiency represents the measured output of the doubler cavity. If mirror M_2 had transmitted all of the generated second harmonic, the observed conversion efficiency would have been 66 percent. In addition, since improper spatial mode matching limited the incoupled power to 92.5 percent of the incident power, the second harmonic generated from the incoupled power represents a 72 percent conversion efficiency.

A small improvement in the doubling efficiency should be possible with even shorter crystals than the 12.5 mm crystal we used. Numerical studies on scaling down the geometry used in our experiments indicate that shorter crystals give improved conversion. A maximum improvement of 10 percent in the second harmonic output power is predicted for a 2 mm long crystal (using a fixed loss of 0.05 percent and a length-dependent loss of 0.15 percent/cm).

The small ring doubler output of 29.7 mW represents a conversion efficiency of 6 percent of the 500 mW diode laser pump power. This efficiency was limited primarily by the design of our Nd:YAG nonplanar ring oscillators. An improved Nd:YAG nonplanar oscillator design that produces 55 mW output from a 150 mW diode laser pump has been developed [25] that would potentially improve the diode laser to green power conversion efficiency by a factor of three.

IV. Summary

We have presented a model for second harmonic generation using an external cavity resonant at the fundamental which takes into account depletion of the circulating power to the second harmonic. Low cavity losses are important for good efficiency so that the dominant loss of the resonated fundamental is to the second harmonic. We have taken advantage of low-loss $MgO:LiNbO_3$ and monolithic designs to efficiently frequency double the output of low-power CW single-axial-mode diode-laser-pumped Nd:YAG lasers. The results of three monolithic cavities were presented and compared to theory. The best efficiency was obtained with a 12.5 mm long ring cavity, which produced 29.7 mW of CW, single axial mode 532 nm radiation from 52.7 mW of incident fundamental for an overall conversion efficiency of 56 percent.

Acknowledgment

We thank Crystal Technology for providing the $MgO:LiNbO_3$.

References

[1] B. Zhou, T. J. Kane, G. J. Dixon, and R. L. Byer, "Efficient, frequency-stable laser-diode-pumped Nd:YAG laser," *Opt. Lett.*, vol. 10, pp. 62–64, Feb. 1985.

[2] R. L. Byer, "Diode pumped solid state lasers," *Science*, vol. 239, pp. 742–747, Feb. 1988; T. Y. Fan and R. L. Byer, "Diode laser-pumped solid-state lasers," *IEEE J. Quantum Electron.*, this issue, pp. 895–912.

[3] T. Y. Fan, G. J. Dixon, and R. L. Byer, "Efficient GaAlAs diode-laser-pumped operation of Nd:YLF at 1.047 μm with intracavity doubling to 523.6 nm," *Opt. Lett.*, vol. 11, pp. 204–206, Apr. 1986.

[4] W. P. Risk, J. C. Baumert, G. C. Bjorkland, F. M. Schellenberg, and W. Lenth, "Generation of blue light by intracavity frequency mixing of the laser and pump radiation of a miniature neodymium:yttrium aluminum garnet laser," *Appl. Phys. Lett.*, vol. 52, pp. 85–87, Jan. 1988.

[5] T. Y. Fan, A. Cordova-Plaza, M. J. F. Digonnet, R. L. Byer, and H. J. Shaw, "Nd:MgO:$LiNbO_3$ spectroscopy and laser devices," *J. Opt. Soc. Amer. B*, vol. 3, pp. 140–147, Jan. 1986.

[6] T. Baer, "Large-amplitude fluctuations due to longitudinal mode coupling in diode-pumped intracavity-doubled Nd:YAG lasers," *J. Opt. Soc. Amer. B*, vol. 3, pp. 1175–1180, Jan. 1986.

[7] A. Ashkin, G. D. Boyd, and J. M. Dziedzic, "Resonant optical second harmonic generation and mixing," *IEEE J. Quantum Electron.*, vol. QE-2, pp. 109–123, June 1966.

[8] T. Y. Fan and R. L. Byer, "Modeling and CW operation of a quasi-three level 946 nm Nd:YAG laser," *IEEE J. Quantum Electron.*, vol. QE-23, pp. 605–612, May 1987.

[9] T. Y. Fan, G. Huber, R. L. Byer, and P. Mitzscherlich, "Continuous wave operation at 2.1 μm of a diode-laser-pumped, Tm-sensitized Ho:$Y_3Al_5O_{12}$ laser at 300 K," *Opt. Lett.*, vol. 12, pp. 678–680, Sept. 1987.

[10] T. J. Kane and R. L. Byer, "Monolithic, unidirectional single-mode Nd:YAG ring laser," *Opt. Lett.*, vol. 10, pp. 65–67, Jan. 1985.

[11] M. Brieger, H. Büsener, A. Hese, F. V. Moers, and A. Renn, "Enhancement of single frequency SHG in a passive ring resonator," *Opt. Commun.*, vol. 38, pp. 423–426, Sept. 1, 1981.

[12] J. C. Bergquist, H. Hemmati, and W. M. Itano, "High power second harmonic generation of 257 nm radiation in an external ring cavity," *Opt. Commun.*, vol. 43, pp. 437–442, Nov. 15, 1982.

[13] J. C. Baumert, J. Hoffnagle, and P. Günter, "High-efficiency intracavity frequency doubling of a steryl-9 dye laser with $KNbO_3$," *Appl. Opt.*, vol. 24, pp. 1299–1301, May 1, 1985.

[14] W. R. Trutna, Jr., D. K. Donald, and M. Nazarathy, "Unidirectional diode-laser pumped Nd:YAG ring laser with a small magnetic field," *Opt. Lett.*, vol. 12, pp. 248–250, Apr. 1987.

[15] J. L. Nightingale, W. J. Silva, G. E. Reade, W. J. Kozlovsky, and R. L. Byer, "Second harmonic generation in MgO doped lithium niobate," in *Proc. SPIE, Vol. 681, Lasers and Nonlinear Opt. Materials*. Bellingham: SPIE, 1987, pp. 20–26.

[16] G. D. Boyd and D. A. Klienman, "Parametric interaction of focused Gaussian beams," *J. Appl. Phys.*, vol. 39, pp. 3597–3639, July 1968.

[17] R. L. Byer, "Parametric oscillators and nonlinear materials," in *Nonlinear Optics*, P. G. Harper and B. S. Wherrett, Eds. San Francisco: 1977, pp. 47–160.

[18] S. K. Kurtz, J. Jerphagnon and M. M. Choy, "Nonlinear dielectric susceptibilities," in *Landolt-Börnstein Numerical Data and Functional Relationships in Science and Technology, Group III: Crystals and Solid State Physics*, vol. 11, K.-H. Hellwege and A. M. Hellwege, Eds. Berlin: Springer Verlag, 1979, pp. 671–743.

[19] T. J. Kane, A. C. Nilsson, and R. L. Byer, "Frequency stability and offset locking of a laser-diode-pumped Nd:YAG monolithic nonplanar ring oscillator," *Opt. Lett.*, vol. 12, pp. 175–177, Mar. 1987.

[20] W. J. Kozlovsky, C. D. Nabors, and R. L. Byer, "Second harmonic generation of a cw diode-pumped Nd:YAG laser using an externally resonant cavity," *Opt. Lett.*, vol. 12, pp. 1014–1016, Dec. 1987.

[21] H. Kogelnik and T. Li, "Laser beams and resonators," *Appl. Opt.*, vol. 5, pp. 1550–1567, Oct. 1966.

[22] T. W. Hänsch and B. Couillaud, "Laser frequency stabilization by polarization spectroscopy of a reflecting reference cavity," *Opt. Commun.*, vol. 35, pp. 441–444, 1980.

[23] R. W. P. Drever, J. L. Hall, F. V. Kowalski, J. Hough, G. M. Ford, A. J. Munley, and H. Ward, "Laser phase and frequency stabilization using an optical resonator," *Appl. Phys. B*, vol. 31, pp. 97–105, 1983.

[24] A. Cordova-Plaza, M. J. F. Digonnet, and H. J. Shaw, "Miniature

CW and actively Q-switched Nd:MgO:$LiNbO_3$," *IEEE J. Quantum Electron.*, vol. QE-23, pp. 262–266, 1987.
[25] T. J. Kane, Lightwave Electronics, Mountain View, CA, private communication.

William J. Kozlovsky was born in 1960. He received the B.S. degree in physics from Loyola University, New Orleans, LA, in 1982, and the M.S. degree in applied physics from Stanford University, Stanford, CA, in 1984.

He is currently pursuing the Ph.D. degree in applied physics at Stanford under support from the Fannie and John Hertz Foundation. His research interests include diode-laser-pumped solid-state lasers and nonlinear frequency conversion of their output.

Mr. Kozlovsky is a student member of the IEEE Lasers and Electro-Optics Society and the Optical Society of America.

C. D. Nabors was born in 1961. He received the S.B. degree in physics from M.I.T., Cambridge, in 1984 where he worked on collision studies in atomic vapors using photon echos, and the M.S. degree in applied physics in 1987 from Stanford University, Stanford, CA, where he is currently pursuing the Ph.D. as a Fannie and John Hertz Foundation Fellow.

His research interests include the use of solid-state lasers for nonlinear and quantum optics applications.

Mr. Nabors is a student member of the IEEE Lasers and Electro-Optics Society and the Optical Society of America.

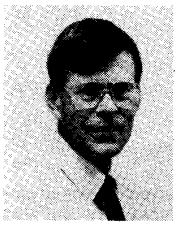

Robert L. Byer (M'75–SM'83–F'87) received the Ph.D. degree in applied physics from Stanford University, Stanford, CA, in 1969.

After joining the Applied Physics Department at Stanford in 1969, he began research in remote sensing using tunable laser sources. Research in that area led to the development of the unstable resonator Nd:YAG laser and to high-power tunable infrared generation in $LiNbO_3$ parametric oscillators. In 1974 he and his colleagues initiated research in coherent anti-Stokes Raman spectroscopy (CARS), named the effect, and extended the research to high resolution, CW CARS spectroscopy in supersonic flows. In 1976 he suggested the use of stimulated Raman scattering in hydrogen gas as a means of generating 16 μm radiation from a CO_2 laser source. Research at Stanford confirmed the expected efficiency of the approach. Research in high-peak and average-power slab geometry solid-state lasers began in 1980. The program led to theoretical and experimental progress in advanced solid-state laser sources. Recent research has centered on diode pumped solid-state laser sources and on the applications of diode-pumped solid-state lasers. His early and continuing interest has been in nonlinear optics and the applications of nonlinear processes to unique measurements. He was Chairman of the Applied Physics Department from 1981 to 1984, Associate Dean of Humanities and Sciences from 1984 to 1987, and is presently Vice Provost and Dean of Research at Stanford. He helped found Quanta Ray Inc. in 1975 and Lightwave Electronics Corporation in 1984. He has published more than 140 technical papers and holds 17 patents in the field of lasers.

Dr. Byer is a member of the National Academy of Engineering and a Fellow of the Optical Society of America. He was President of the IEEE Lasers and Electrooptics Society in 1985.